Article ID: 1003－6326(2004)01－0184－06

Modeling of thermal conductivity of stainless-steelmaking dust pellets①

PENG Bing(彭 兵)[1], PENG Ji(彭 及)[1], YU Di(余 笛)[2]
(1. School of Metallurgical Science and Engineering, Central South University, Changsha 410083, China;
2. School of Information Science and Engineering, Central South University, Changsha 410083, China)

Abstract: The thermal conductivity of stainless-steelmaking dust pellets, an important parameter for the direct recycling of the dust, is naturally of interest to metallurgists. The measurement of central temperature and surface temperature was taken in a furnace. The physical model and calculation model for the heating process were set up to check the thermal conductivity of the dust pellets. The physical structure parameters δ and λ of the basic unit are 0.92 and 0.45 based on the calculation. The temperature in the pellet can be expressed in a linear equation $a_5T_P = a_1T_N + a_2T_M + a_4$. This is convenient to determine the central temperature of a pellet in the direct recycling process.

Key words: thermal conduction; stainless-steelmaking dust; recycling
CLC number: TF 741.5 **Document code:** A

1 INTRODUCTION

In a typical stainless-steelmaking operation, the temperature generally reaches 1 600 ℃ or higher. Approximately 1%－2% (mass fraction) of the scrap charged to the smelting furnaces is converted into dust under these conditions[1]. All of the zinc, lead and cadmium present in the charge enter into the gas phase. At the same time, the high temperatures and turbulence in the smelting furnace cause a lot of iron, chromium and nickel to volatilize. As the metal vapors exit from the furnace and the temperature drops, the fumes are oxidized and condensed. Complex microscopic agglomerates form physically and chemically on condensed nuclei such as fugitive dust particles and then are collected as particulate matter in the baghouse system. This dust is considered a by-product of steelmaking process. When being stockpiled, the heavy metals in the dust are leached by the groundwater in concentrations that exceed provincial environmental guidelines, which makes the dust assigned a hazardous waste and be banned from landfills by various government regulatory agencies. In addition, the dust is also an economical material for the stainless-steelmakers as it contains large amount of valuable metals such as chromium and nickel.

Direct recycling of stainless-steelmaking dust was conducted in previous researches[2]. It is a remediation option to recover the metallic elements present in the dust directly to the steel bath[3, 4]. The dust is mixed with a reducing agent carbon firstly and then formed into pellets that are subsequently fed to the smelting furnace. Under the conditions in the furnace, it is convenient to reduce the metal oxides in the dust by carbon and recover the reduced metals into the steel melt as the alloying elements. This is a self-reducing process. In order to do so, the characteristics of the dust were investigated[5], and the isothermal[6] and non-isothermal[7, 8] kinetic models of the reduction of the pellets were established. It was also found that the thermal conductivity of the pellets greatly influences the reduction process, which depends on the temperature, porosity of the pellets and percentage of reduced metals. Ding et al[9] indicated that thermal conduction controls the process in the beginning of reduction instead of kinetic conditions. Akiyama et al[10, 11] noticed that the contact of particles inside a pellet should be considered for the better expression of effective thermal conductivity of a porous pellets after modifying Luikov model. In his work, each unit cell was composed of core and connecting parts. The core was represented by a cube and the connecting parts were composed of three bars. But it seems different from the effective thermal conductivity of the porous and metallized pellet for the evaluation of its heating and melting in the direct recycling of stainless-steelmaking dust. This paper focuses on modeling of the thermal conductivity of stainless-steelmaking dust pellets.

2 EXPERIMENTAL

2.1 Experimental materials

The stainless-steelmaking dust for the experiment was taken from a stockpile located in the open

① **Foundation item:** Project(50274073) supported by the National Natural Science Foundation of China
Received date: 2003－04－10; **Accepted date:** 2003－07－23
Correspondence: PENG Bing, Professor, PhD; Tel: +86-731-8830875; E-mail: pengyu@public.cs.hn.cn

air. As it was exposed to the atmosphere, the dust contained a large amount of moisture that caused particles to agglomerate over time. The particle sizes of the dust samples were in a very wide range from less than 38 μm to approximately 5 cm. Elemental analysis of dust samples was performed using X-ray Fluorescence (XRF) for Al, Ca, Cr, Fe, K, Mg, Mn, Na, P, Si, Ti and Inductively Coupled Plasma (ICP) for Ni, Pb and Zn. The compositions of the samples are given in Table 1. Since the dust was formed in air at high temperature, most of the elements within it were oxidized. X-ray Diffraction (XRD) analyses indicated that the main phases present in the dust were Fe_3O_4, Fe_2O_3 and CrO, which are given in Table 2.

Table 1 Composition of electric arc furnace dusts (Mass fraction, %)

Al	Ca	Cr	Fe	K	Mg	Mn
0.41	6.13	10.60	39.12	0.15	5.96	8.36
Na	Ni	P	Pb	Si	Ti	Zn
0.17	3.92	0.02	0.12	2.64	0.14	0.59

Table 2 Main phases of electric arc furnace dust (Mass fraction, %)

SiO_2	Al_2O_3	CaO	CrO	Fe_2O_3
5.45	0.66	9.14	13.51	58.00
MnO_2	NiO	PbO	ZnO	MgO
4.67	6.70	0.16	0.93	3.48

The dust was crushed in a ball miller for about 20 min and then screened to < 0.4 mm in order to be suitable for pelletization. The carbon particles used as the reducing agent in the pellets were finer than 38 μm. The pellets were made from the mixture of 80% dust+ 15% carbon+ 5% binder(mass fraction) using a disc pelletizer. The pellets agglomerated with a diameter of about 10 mm were dried in air at room temperature for 4 d. The SEM observation for the central section of the pellets is shown in Fig. 1.

2.2 Experimental approach

The apparatus for the experiment used in this study is shown in Fig. 2. Nitrogen was introduced to the furnace in case that the air got in. The temperature on the surface and at the cross-section of pellet was detected by the thermocouples. One alumina tube with a thermocouple was fixed 1 mm under the surface and the other at the center of the pellet. After preheating the furnace to 1 500 ℃, the pellet in an empty crucible was put into the furnace. The temperature of the pellet surface and center was measured and recorded continuously during the experiment. These measurements of temperature are beneficial for the explanation of heat transfer inside the pellet and for modeling the heat transfer process and thermal conductivity of the pellet.

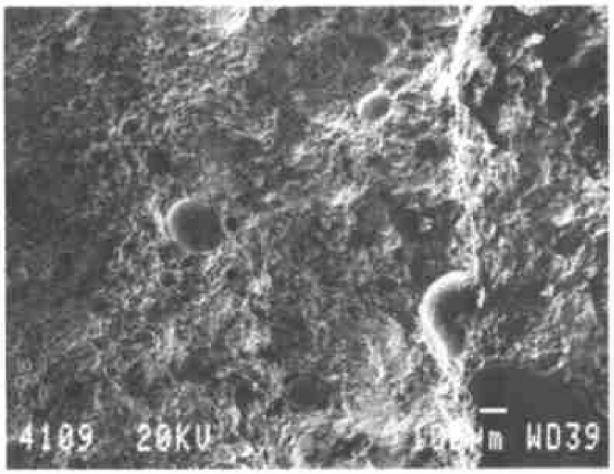

Fig. 1 SEM image of central section of pellets

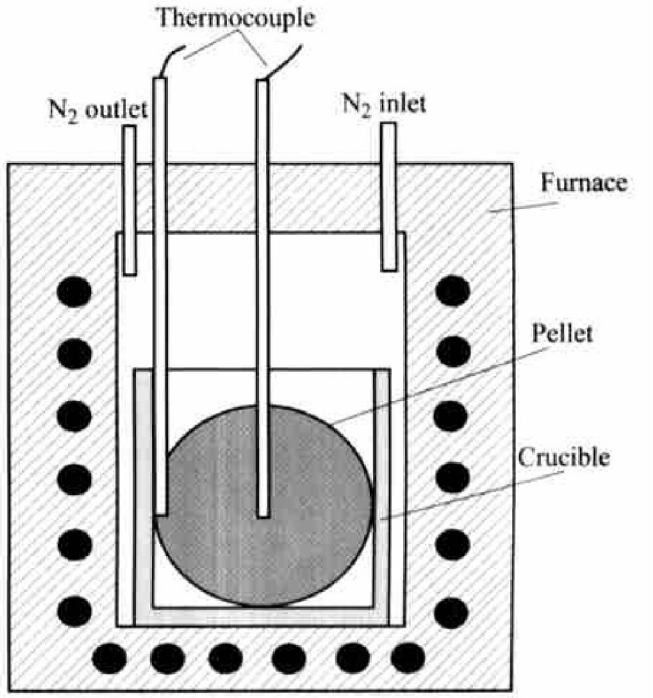

Fig. 2 Sketch of experimental apparatus

3 EXPERIMENTAL RESULTS

Fig. 3 shows the temperature measured at the surface and the center of pellet and their difference as the function of time in the experiment. It is the main features of the temperature curves in the pellet heating process. It can be seen from the figure that the surface temperature rose faster than that at the center when the pellet was heated up and a temperature gradient was formed from the surface to the center of the

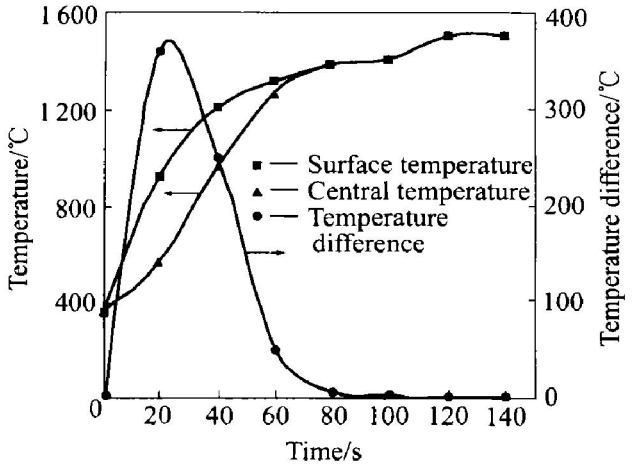

Fig. 3 Change of temperature at surface and center of pellet

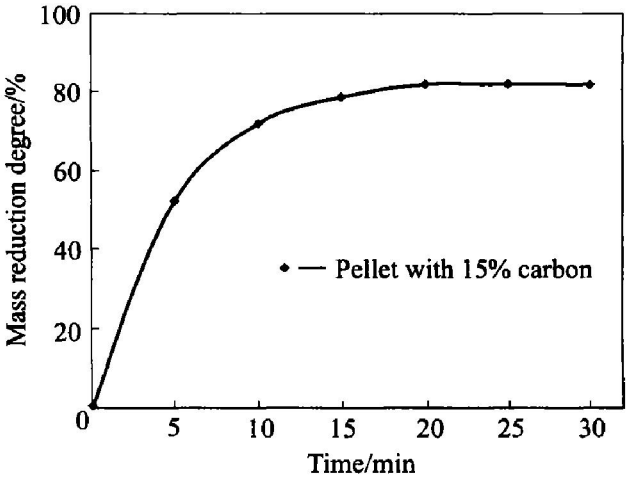

Fig. 4 Profile of mass reduction degree of pellet vs time

pellet. After that, the temperature difference increased and reached a maximum value. The temperature difference only existed in the beginning 80 s of the reduction process. At the end, the temperature of the pellet reached the surrounding temperature of the furnace.

In order to check the influence of the reduction degree on the pellet thermal conductivity, the mass change profile in the reduction process was recorded in exactly the same experimental condition. The reduction degree of the pellet in the heating process was calculated according to the removed oxygen in the dust. The reduction degree $R(t)$ can be expressed as

$$R(t) = (m_0 - m_t)/\Delta m_\Sigma$$

where m_0 represents the initial mass of the pellet, m_t the pellet mass at time t, Δm_Σ the maxim possible mass loss in the reduction process.

The calculation result of reduction degree vs time is shown in Fig. 4. The central temperature of the pellet will be strongly speeded up by increasing the reduction degree, which results from improved heat conductivity. The temperature difference between the center and surface of pellet in the heating process happened in the beginning of the reduction. Most of metal oxides present in the dust were reduced by the carbon in the homogeneous temperature condition.

4 THERMAL CONDUCTION MODEL

4.1 Physical model

To develop a controlling technique of steelmaking process, many accurate data are required. The thermal conductivity of stainless-steelmaking dust pellets, an important parameter for the direct recycling run, is naturally of interest to steelmakers. Since the pellets are multi-component and porous materials, it is important to find proper expression of their effective thermal conductivity. It could be imagined that the effective thermal conductivity of a porous medium has to include the effect of the conductivity of the solid phase and the gas phase, as well as the porosity of the medium. Akiyama et al[12] delivered an expression of effective thermal conductivity of porous pellet in 1992:

$$k_e = ek_g + (1-e)k_s \quad (2)$$

where k_e stands for the effective thermal conductivity; e the porosity of pellet, %; k_g the thermal conductivity of the gas phase and k_s the thermal conductivity of solid phase. This expression contained only effects of two phases, metal oxides and porosity, and only took the porosity as a structure parameter. In their work, a unit model, which was originally proposed by Luikov[11] for describing the continuity of porous materials, was used, as shown in Fig. 5. In this model, each unit cell was composed of core and connecting parts. A cube and the connecting parts represented the core. The structure were evaluated by parameters $\theta(0 \leqslant \theta \leqslant 1)$ and $\xi(0 \leqslant \xi \leqslant 1)$. The porosity in this model was expressed as

$$e = 1 - \theta^3 - 3(\xi\theta)^2(1-\theta) \quad (3)$$

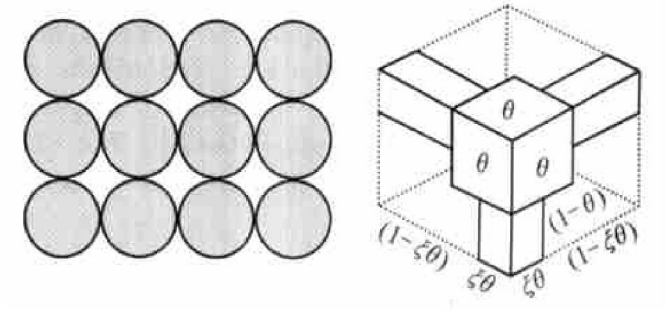

Fig. 5 Physical model of effective coductivity of porous pellet by Akiyama[12]

In practical direct recycling process, porous pellets have very different structures even if they might have the same porosity. The reduced metallic metals

will cause the structural to change in the pellets. It is necessary to build a much complicated and realistic physical model instead of simple expressions. A new modified physical model is adopted in this study to describe the structure and effective thermal conductivity of the metallized porous pellet, and to evaluate their heating and melting process based on the experimental work and results. As shown in Fig. 6, the unit cells of the pellets are in the globe shape instead of cube and the elementary cells contain either reduced metals and pores or metal oxides and pores. Both reduced metal cells and metal oxide cells are randomly distributed inside the pellets. Each cell consists of a spherical core at the center and six cylindrical arms connected with other cells. This model is much closer to the reality and easier to emulate the melting process than that by Akiyama. The radii of the cell core $\delta(0 \leqslant \delta \leqslant 1)$ and arm $\lambda(0 \leqslant \lambda \leqslant 1)$ are used as the pellet structure parameters. The porosity of pellets in the new model can be expressed as

$$e = 1 - (1/6)\pi\delta^3 - (3/4)\pi\lambda^2(1-\delta) \quad (4)$$

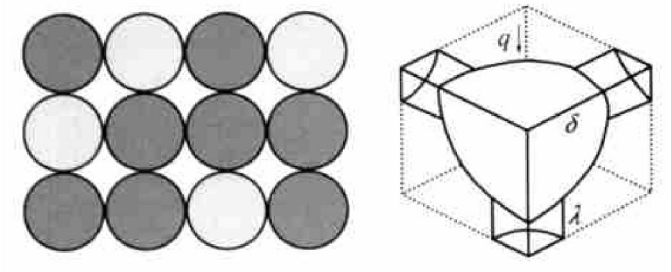

Fig. 6 Physical model of effective conductivity of porous pellet used in this study

4.2 Calculation model

On the basis of physical model above, the calculation in this study was concentrated on the expression for the effective thermal conductivity by means of the structural parameters δ and λ, expression for the temperature fields inside the pellet and partially differential equation of unsteady heat transfer and its numerical solution.

The porosity of the pellets used in this study was in the range of 50% - 60%. Fig. 7 shows the relationship between the radius of unit core and that of unit arm. It was determined by the certain pellet porosity in the pellet smelting temperature range of 400 - 1 300 ℃. A larger core radius can result in a small unit arm. The radius δ varied in the range of 0.7 - 0.95 and the unit arm radius λ decreased from 0.75 to zero correspondingly. It is because the unit arm is the connecting part of the elementary cells in which a large arm represents tight contacts of the particles inside the pellet and high thermal conductivity consequently. Naturally, small arms in the unit cell indicate loose connections of particles inside the pellet and low thermal conductivity as well.

According to Patankar's equation[12], the basic

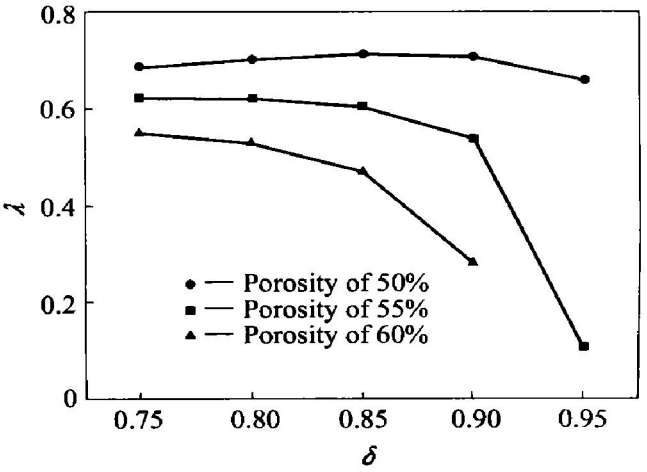

Fig. 7 Relationship of unit core radius with unit arm radius

equation of unsteady heat conduction in a spheroidal coordination and the boundary conditions were as follows:

$$\rho_p \frac{\partial T}{\partial t} = \frac{1}{r^2}\frac{\partial}{\partial r}\left(r^2 k_e \frac{\partial T}{\partial r}\right) + q \quad (5)$$

$$T_s = S(t)$$

$$\left.\frac{\partial T}{\partial r}\right|_{r=0} = 0$$

where ρ stands for the apparent density of the pellet, kg/m^3; c_p the apparent heat capacity of the pellet, J/(kg·K); T the temperature, K; t the time, s; r position along the pellet radius, m; k_e the effective thermal conductivity, W/(m·K); q the heat flux from the source, J/(m^3·s); T_s the temperature at the pellet surface; and $S(t)$ the pellet surface temperature function with time.

The heat produced inside the pellet in the beginning of the heating could be neglected because there was not so much temperature reduction happened at this time. A infinite difference method was adopted to solve Eqn. (5) numerically and the boundary condition $T_s = S(t)$ came from the experimental results. The calculation was carried out by integrating Eqn. (5) over the controlled volume shown in Fig. 8, in distance range from m to n and time period from t to $t + \Delta t$:

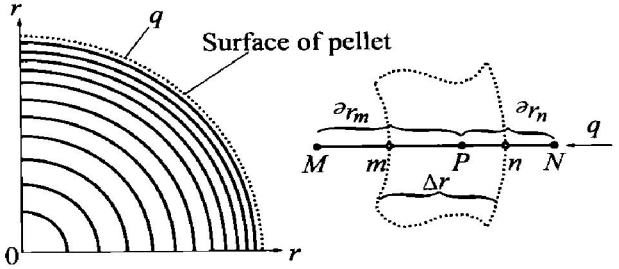

Fig. 8 Integration area along pellet radius

$$\rho c_p \int_m^n \int_t^{t+\Delta t} r^2 \frac{\partial T}{\partial t} \mathrm{d}r\,\mathrm{d}t = \int_m^n r^2 \mathrm{d}r \int_t^{t+\Delta t} k_e \frac{\partial T}{\partial t} \mathrm{d}t + q \int_m^n \int_t^{t+\Delta t} r^2 \mathrm{d}r\,\mathrm{d}t \quad (6)$$

Integrating the left side of Eqn. (6), the equation could be expressed as follows:

$$\rho c_p \int_n \int^{\Delta t} r^2 \frac{\partial T}{\partial t} \mathrm{d}r\,\mathrm{d}t = \frac{1}{3}\rho\ c_p (n^3 - m^3)(T_{p2} - T_{p1}) \quad (7)$$

where T_{p1} is the temperature at point P and t moment; T_{p2} is the temperature at point P and $t + \Delta t$ moment. Then, integrate the right side of Eqn. (6) and it could be expressed as:

$$\int_n r^2 \mathrm{d}r \int^{\Delta t} k_e \frac{\partial T}{\partial t} \mathrm{d}t + q \int_n \int^{\Delta t} r^2 \mathrm{d}r\,\mathrm{d}t = \int^{\Delta t} [n^2 k_{e,n} (T_m - T_p)/(\partial r)_n - m^2 k_{e,m} \cdot (T_p - T_m)/(\partial r)_m] \mathrm{d}t + \frac{1}{3} q (n^3 - m^3) \Delta t \quad (8)$$

Up to now, the integration form of Eqn. (6) in the controlled volume and time interval could be written as follows. And in a short time period Δt, the temperature T_m at the point m and the temperature T_p at the point p as well as the temperature T_m at the point m will not change with time t:

$$\frac{1}{3}\rho c_p (n^3 - m^3)(T_{p2} - T_{p1}) = \int^{\Delta t} [n^2 k_{e,n} (T_m - T_p)/(\partial r)_n - m^2 k_{e,m} \cdot (T_p - T_m)/(\partial r)_m] \mathrm{d}t + \frac{1}{3} q (n^3 - m^3) \Delta t = [n^2 k_{e,n} (T_m - T_p)/(\partial r)_n - m^2 k_{e,m} \cdot (T_p - T_m)/(\partial r)_m] \Delta t + \frac{1}{3} q (n^3 - m^3) \Delta t$$

Let $a_1 = n^2 k_{e,n}/(\partial r)_n$; $a_2 = m^2 k_{e,m}/(\partial r)_m$; $a_3 = \frac{1}{3}\rho c_P \Delta t (n^3 - m^3)$; $a_4 = \frac{1}{3} q (n^3 - m^3) + a_3 T_{p1}$;

$a_5 = a_1 + a_2 + a_3$, then the final linear expression can be obtained by rewriting Eqn. (9) as follows:

$$a_5 T_P = a_1 T_N + a_2 T_M + a_4 \quad (10)$$

5 CALCULATION RESULTS AND DISCUSSION

In this study, the pellet properties and temperature measured was used as the input data. A computer program was developed to output the variations of the central temperature of pellet and the radii of the core and arm of the unit cell. In the program the calculation results were also compared with the experimental ones to minimize the differences. The experimental temperature measurements at the pellet surface were taken as the boundary conditions and the central temperature measurements were used to evaluate the calculation results. The temperature difference between the center and surface of pellet happened in the first 80 s of the heating(Fig. 3). The proportion of reduced metals was very low and would not make the structure parameters δ and λ of the pellet change so much. The structure parameters of porous pellets in this study are listed in Table 3 . It should be mentioned that the unit arm represents the connection of solid particles inside the pellets and small arm will have negative effect on the heat transfer.

Table 3 Structure parameters of porous pellets

Mass reduction degree of pellet/ %	Pellet porosity/ %	Radius of unit core, δ	Radius of unit arm, λ
0 - 3.2	55.43	0.92	0.45

Fig. 9 gives the calculation results and the comparison of the pellet central temperature calculated by the developed model with the experimental results. It shows a good agreement of calculation results with the experimental results even though the parameters ρ, c_p, e and k_e changed in the heating process.

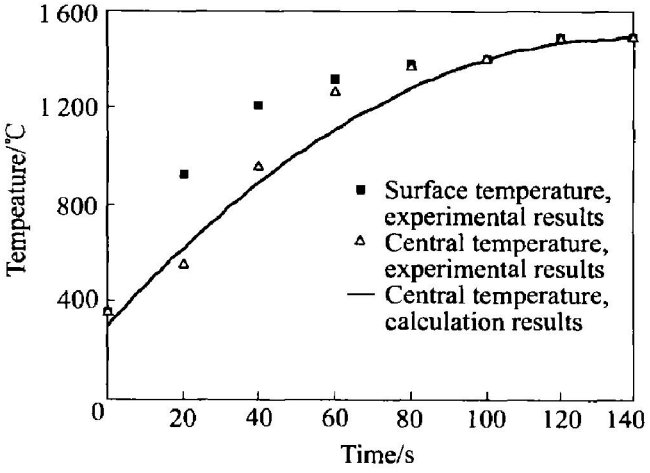

Fig. 9 Comparison of calculation results and experimental results

The direct recycling of stainless-steelmaking dust is a new process. Modeling the heating process in this study could deliver some basic properties of the pellets that determine their melting behaviors.

6 CONCLUSIONS

1) The physical model developed in this study is based on previous work by Luikov and Akiyama. But a spherical core and cylindrical arms is used and make the model closer to reality. The parameters δ and λ of physical model are determined as 0.92 and 0.45 respectively in a three-dimensional unit. In this modified unit cell model, the combination of the radius of unit core and that of connection arm can represent the porosity of the pellets. The connection arm in this model also represents the contact between solid particles inside the pellets, which is very important for the heat transfer capacity of the porous pellets.

2) The temperature in the pellet has a linear expression of $a_5 T_P = a_1 T_N + a_2 T_M + a_4$. The calcula-

tion results fit the experimental results fairly well in the case of pellet central temperature variation.

REFERENCES

[1] Zunkel D. What to do with your EAF dust[J]. Steel Times International, 1996, 20(4): 46 - 50.

[2] Zhang C F, Peng B, Peng J, et al. The direct recycling of electric arc furnace stainless-steelmaking dust[A]. The 6th International Symposium on East Asian Resources Recycling Technology[C]. Gyeongiu, Korea, The Korean Institute of Resources Recycling: 2001. 404 - 408.

[3] PENG Bing, PENG Ji, Kozinski J A, et al. Thermodynamic calculation on the smelting slag of direct recycling of electric arc furnace stainless-steelmaking dust [J]. Journal of Central South University of Technology, 2003, 10(1): 20 - 26.

[4] Lobel J, Peng J, Bourassa M, et al. Pilot-scale direct recycling of flue dust generated in electric stainless-steelmaking[J]. Iron and Steelmaker, 2000, 27 (1): 41 - 45.

[5] Souza N D, Kozinski J A, Szpunar J A. EAF stainless steel dust, characteristics and potential metal immobilization by thermal treatment[A]. International Symposium on Resource Conservation and Environmental Technology in the Metallurgical Industry[C]. Calgary, Alberta, 1998.

[6] PENG B, ZHANG C, PENG J, et al. Kinetics research of EAF dust reduction in isothermal condition[J]. Journal of Anhui University of Technology, 2000, 18(1): 13 - 17. (in Chinese)

[7] ZHANG C F, PENG B, PENG J, et al. Electric arc furnace dust non-isothermal reduction kinetics [J]. The Chinese Journal of Nonferrous Metals, 2000, 10(4): 524 - 530. (in Chinese)

[8] PENG B, Lobel J, Kozhinski J A, et al. Non-isothermal reduction kinetics of EAF dust-based pellets[J]. Cim Bulletin, 2001, 94 (1049): 64 - 70.

[9] Ding Y L, Warner N A, Merchant A J. Mathematical modelling of the reduction of carbon-chromite composite pellets[J]. Scandinavian Journal of Metallurgy (Denmark), 1997, 26(1): 1 - 8.

[10] Akiyama T, Ohta H, Takahashi R, et al. Measurement and modeling of thermal conductivity for dense iron oxide and porous iron ore agglomerates in stepwise reduction[J]. ISIJ International, 1992, 32(7): 829 - 837.

[11] Luikov A, Ohta H, Vasiliev L, et al. Thermal conductivity of porous systems[J]. Heat Mass Transformation, 1968, 11(1): 117 - 140.

(Edited by YANG Bing)